doi:10.3772/j.issn.1006-6748.2015.04.001

Adaptive friction compensation for large diameter electro-hydraulic proportional valve cores based on LuGre①

Kong Xiangdong (孔祥东)②[*,**,***], Song Yu[***], Ai Chao[***], Li Yanpeng[***], Tian Dezhi[***]

([*] Key Laboratory of Advanced Forging & Stamping Technology and Science (Yanshan University), Ministry of Education of China, Qinhuangdao 066004, P. R. China)

([**] Hebei Provincial Key Laboratory of Heavy Machinery Fluid Power Transmission and Control, Yanshan University, Qinhuangdao 066004, P. R. China)

([***] School of Mechanical Engineering, Yanshan University, Qinhuangdao 066004, P. R. China)

Abstract

This paper presents an adaptive friction compensation method based on LuGre model for large diameter electric-hydraulic proportional valves in which the valve core contains friction. A mathematic model of the electric-hydraulic proportional valve is established, and the friction characteristics are described based on the LuGre model. The global asymptotic stability of the control system with the adaptive friction compensation controller is guaranteed over Lyapunov theorem. The adaptive compensation of the friction on LuGre friction model is verified by simulation and experiment. The steady-state error is about $[-4.23\times10^{-5}\text{m}, 5.91\times10^{-5}\text{m}]$ and $[-2.5\times10^{-4}\text{m}, 2.6\times10^{-4}\text{m}]$ on simulation and experiment, the position tracking accuracy is higher, and the lag time of the main valve through the dead zone is shorter. The result proves that the adaptive friction compensation method can effectively compensate for the negative effects of nonlinear friction.

Key words: electric-hydraulic proportional valve, pilot stage, LuGre, adaptive friction compensation, experimental identification

0 Introduction

As the requirement for hydraulic control system increases gradually, higher requirements are put forward for the electro-hydraulic proportional valve[1]. Research institutions and scholars have promoted the static and dynamic characteristics of the proportional valve by improving the working principle and structure all around the world. Due to the friction characteristics of valve cores, the flow characteristics of valve port and the hysteresis characteristics of coil of the proportional valve, the proportional valve core cannot get accurate displacement control and limits the precision of the control system. Among them, the nonlinear friction characteristic of the valve core is the most important influence factor. The existence of the nonlinear friction leads to the limit cycle oscillation and low speed crawl phenomenon, therefore the static and dynamic characteristics of the proportional valve are affected badly. Reducing the negative impact of the valve core friction is an effective way to improve the proportional valve's dynamic and static performance.

Based on the structure of optimizing valve core, the nonlinear friction compensation also attracts extensive attention[2]. When the radial force of the proportional valve core is balanced, valve core and valve body fluid port are completely concentric and the clearance around is uniformly distributed between valve core and valve body, only friction caused by Newtonian fluid shear force exists. However, in engineering, certain shape error and deformation exists in valve core and valve body fluid port, inevitably the valve core radial hydraulic pressure distribution is not uniform, and a large numerical friction is formed. Friction is a function of velocity discontinuity, and it is the main factor of high precision motion control[3,4]. Therefore, to improve the performance of proportional valve, the appropriate control method must eliminate the influence of friction.

Nonlinear PID control strategy is a common compensation method. Adjusting the PID parameters by the

① Supported by the National Key Basic Research Program of China (No. 2014CB046405), Key Projects in the National Science & Technology Pillar Program during the Twelfth Five-year Plan of China (No. 2014BAF02B00, 2011BAF09B04).

② To whom correspondence should be addressed. E-mail: xdkong@ysu.edu.cn

Received on Oct. 11, 2014

working state is better to restrain friction, such as analyzing PID control for valve-controlled hydraulic motor positioning control system[5], and friction compensation for the electric cylinder[6]. With the integral element, PID control can eliminate system static error theoretically, but low speed friction nonlinear characteristics, the memory of integral element will lead to the emergence of the limit cycle in position control system. In the following control system, when speed steering happens, the integral loop will lead output torque and static friction to get into the same direction, so as to increase the influence of friction[7]. At present, domestic and foreign scholars put forward some adaptive friction compensation methods, one example is that the coulomb friction is expressed as a function of time, and making up for the defects of fixed coulomb friction model by improving the observer gain[8]. Another method is to present the observer gain as a function of velocity, and the constraint condition of gain function is deduced by Lyapunov function[9]. However, the friction model based on velocity function can't describe the nonlinear characteristic of friction in static, and the control effect is limited. With the consideration of Stribeck effect in compensation method, a more precise description of the friction phenomenon[10] is given to the ultra-low speed period. Since the above friction model is the static one and its dynamic characteristic of friction compensation effect is limited, its application is restricted.

The LuGre friction model is a relatively complete dynamic friction model. All kinds of static and dynamic characteristics of friction can be accurately described, which has become a hotspot in the research of theory and application[11-13]. Basically, the adaptive control strategy of friction is designed on the basis of Layapunov stability proved in this paper, which enables adaptive compensation of the friction on LuGre friction model.

1 Mathematics model of electro-hydraulic proportional valve

1.1 Mathematics model of hydraulic proportional valve

The hydraulic principle diagram of large diameter electro-hydraulic proportional valve is shown in Fig. 1. It comprises of a proportional amplifier, a pilot stage, a relief valve and a main stage. According to the principle diagram, the mathematical model of the components is established.

1) The proportional amplifier: The proportional amplifier is used to regulate the electro-hydraulic proportional valve which is an important unit. The mathematical model is described by

$$i = \left(k_s\left(e + \frac{1}{T_i}\int_0^t e\mathrm{d}t + T_d\frac{\mathrm{d}e}{\mathrm{d}t}\right) + u_i + u_d\right)k_a \quad (1)$$

where, i is the driven current of the proportional electromagnet, k_s is proportional coefficient, e is the input deviation signal, T_i is the integration time constant, T_d is the differential time constant, k_a is the power amplification coefficient, u_i is the bias current, u_d is the amplitude of chatter signal.

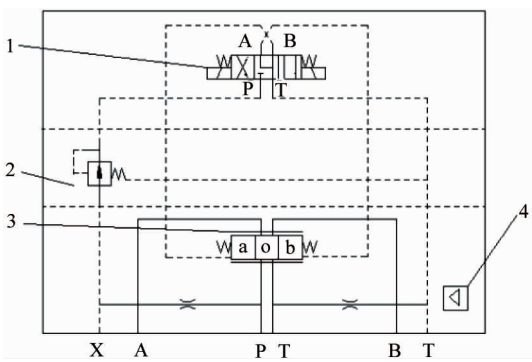

1 The pilot stage; 2 The main stage; 3 The relief valve; 4 The proportional amplifier

Fig. 1 The hydraulic principle diagram of large diameter electro-hydraulic proportional valve

2) The pilot stage: The pilot stage uses direct proportional direction throttle valve in this paper. The valve core of power level is driven by the proportional electromagnet directly, and the flow rate and direction are controlled.

The proportional electromagnet is described by

$$F_{ph} = k_e i \quad (2)$$

where, F_{ph} is the force of the proportional electromagnet, k_e is the conversion coefficient of the proportional electromagnet.

The force equilibrium equation of pilot valve is described by

$$F_{ph} = m_p\frac{\mathrm{d}^2x_p}{\mathrm{d}t^2} + B_{pp}\frac{\mathrm{d}x_p}{\mathrm{d}t} + 2k_{pk}x_p + F_{ps} + F_{pt} + F_{pf} \quad (3)$$

where, m_p is the pilot valve core and the equivalent mass in the pilot valve, x_p is the displacement of the pilot valve, B_{pp} is the viscosity damping coefficient of the pilot valve, k_{pk} is the centered spring rigidity of the pilot valve, F_{pt} is the steady-state fluid force of the pilot valve, F_{pt} is the transient flow force of the pilot valve, and F_{pf} is the friction force of the pilot valve.

According to the pilot valve core and valve body dimension relations, the pilot valve opening degree is described by

$$x_{pi} = \begin{cases} x_p + x_{piv} & -x_{ps} \leqslant x_p \leqslant -x_{piv} \\ 0 & x_p < |x_{piv}| \\ x_p - x_{piv} & x_{piv} \leqslant x_p \leqslant x_{ps} \end{cases} \quad (4)$$

where, x_{pi} is the opening degree of the pilot valve port i, x_{piv} is the overlap degree of the pilot valve port i, x_{ps} is the maximum displacement of the pilot valve.

The flow equation is described by

$$q_L = k_q x_{pi} - k_c p_L \quad (5)$$

where, q_L is the load flow of the pilot valve, p_L is the load pressure of the pilot valve, k_q is the flow gain, k_c is the pressure gain.

3) The main stage: The flow continuity equation of the main valve is described by

$$q_L = A_m \frac{\mathrm{d}x_m}{\mathrm{d}t} + C_{tp} p_L + \frac{V_t}{4\beta_e} \frac{\mathrm{d}p_L}{\mathrm{d}t} \quad (6)$$

where, A_m is the efficient working area of the main valve, x_m is the displacement of the main valve core, C_{tp} is the integrated leakage coefficients, V_t is the total compressed volume and β_e is the effective volume elastic modulus.

The force equilibrium equation of the main valve is described by

$$A_m p_L = m_m \frac{\mathrm{d}^2 x_m}{\mathrm{d}t^2} + B_{mp} \frac{\mathrm{d}x_m}{\mathrm{d}t} + k_{mk} x_m + F_{mk0} + F_{ms} + F_{mt} + F_{mf} \quad (7)$$

where, m_m is the main valve core and the equivalent mass in the pilot valve, B_{mp} is the viscosity damping coefficient of the main valve, k_{mk} is the centered spring rigidity of the main valve, F_{mk0} is the pre-tightening force of the centered spring, F_{ms} is the steady-state fluid force of the main valve, F_{mt} is the transient flow force of the main valve and F_{mf} is the friction force of the main valve.

4) The displacement sensor: The linear variable differential transformer (LVDT) and modulation-demodulation measuring and amplifying circuit are adopted in this paper. The mathematical model is described by

$$u_f = k_{md} x_m \quad (8)$$

where, u_f is the feedback voltage of the displacement sensor, k_{md} is the conversion coefficient of the displacement amplifier circuit.

According to the mathematical model of components, the block diagram of large diameter electro-hydraulic proportional valve is concluded and shown in Fig. 2.

The pilot valve controlling main valve is the typical valve control cylinder model with elastic load, the spring- quality-damping system is composed of hydraulic spring, centralizing spring and the mass of main valve. The simplified model of the main valve output displacement is shown in Eq. (9).

$$X_m = \frac{\frac{k_p A_m}{k_{mk}} X_{pi} - \frac{1}{k_{mk}}\left(1 + \frac{V_t}{4\beta_e k_{ce}} s\right)(F_{mk0} + F_{ms} + F_{mt} + F_{mf})}{\left(\frac{s}{w_r} + 1\right)\left(\frac{s^2}{w_0^2} + \frac{2\zeta_0}{w_0} s + 1\right)} \quad (9)$$

where, k_{ce} is the flow-pressure coefficient, $k_{ce} = k_c + C_{tp}$, k_p is the pressure gain, $k_p = k_q / k_{ce}$, w_r is the turning frequency of the pilot valve controlling main valve, ζ_0 is the integrated damping ratio of the pilot valve control the main valve.

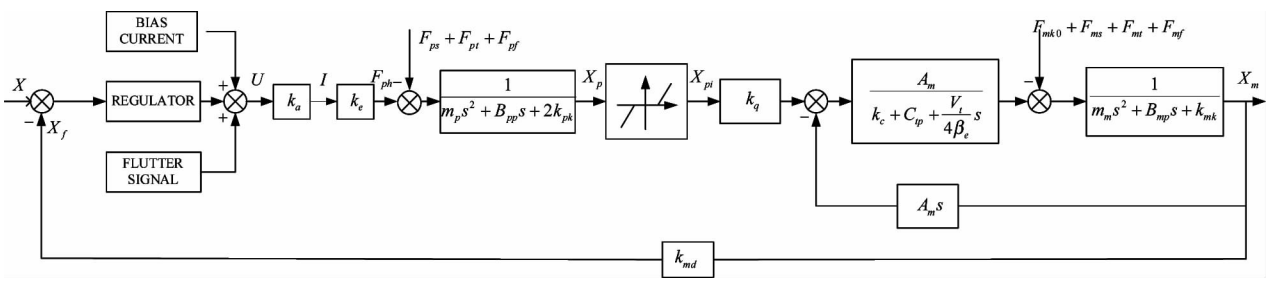

Fig. 2 The block diagram of the piloted large diameter electro-hydraulic proportional valve block diagram

1.2 The LuGre model

From relatively static to the relative motion, four experienced stages of the friction of the main valve core are the stage of interface elastic deformation, the stage of boundary lubrication, the stage of partial fluid lubrication and the stage of completely fluid lubrication. In these four stages, the friction and the relative velocity are in steady-state corresponding relationship between contact surfaces, namely the Stribeck model, and the curve is shown in Fig. 3.

The steady-state of the LuGre model is consistent with the Stribeck model, which is a relatively complete dynamic model, and the static and dynamic characteristics of nonlinear friction can be described and predicted accurately, and the dynamic compensation effect of the friction is better[14]. In dynamic the LuGre model

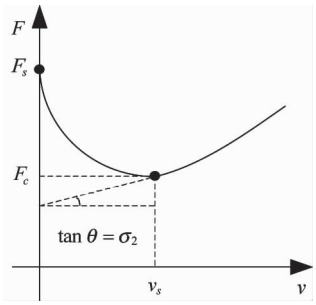

Fig. 3 The curve of the Stribeck

regards the friction contact surface as elastic mane with stochastic behavior in microscopic[15].

The friction of LuGre model is produced by the mane of deflection, the parameters of which are shown in Eqs(10) ~ (12).

$$F_f = \sigma_0 z + \sigma_1 \frac{\mathrm{d}z}{\mathrm{d}t} + \sigma_2 v \tag{10}$$

$$\frac{\mathrm{d}z}{\mathrm{d}t} = v - \frac{|v|}{g(v)} z \tag{11}$$

$$\sigma_0 g(v) = F_c + (F_s - F_c) e^{-(v/v_s)^2} \tag{12}$$

where, σ_0 is the friction rigidity coefficient, z is the average deformation of the bristle, σ_1 is the damping coefficient of the friction, σ_2 is the viscous friction coefficient, F_c is the coulomb friction force, F_s is the static friction force, v_s is the critical velocity of Stribeck, v is the valve core velocity, $g(v)$ is a bounded function more than zero.

2 Design of the friction compensation controller

The large diameter electro-hydraulic proportional valve control system monitors the performance and parameters of a controlled object with friction compensation controller, and feeds back acquisition data to the controller, then makes the proportional valve system work in optimal state. When the friction compensation controller is designed, this paper assumes that the special-shaped composite non-circular opening valve has reduced the fluid force of the main valve, and viscous damping coefficient is neglected. Eq. (7) has been simplified, thus the force equilibrium equation of main valve is described by

$$A_m p_L = m_m \frac{\mathrm{d}^2 x_m}{\mathrm{d}t^2} + k_{mk} x_m + F_{mk0} + F_{mf} \tag{13}$$

By linking Eq. (13) with Eqs(10) and (11), the LuGre model is described by

$$m_m \ddot{x}_m = F_{mh} - \sigma \dot{x}_m - k_{mk} x_m - \sigma_0 z + \sigma_1 \frac{|\dot{x}_m|}{g(\dot{x}_m)} z - F_{mk0} \tag{14}$$

where, $\sigma = \sigma_1 + \sigma_2 > 0$.

The observer equation is described by

$$\frac{\mathrm{d}\hat{z}_0}{\mathrm{d}t} = \dot{x}_m - \frac{|\dot{x}_m|}{g(\dot{x}_m)} \hat{z}_0 + l_0 \tag{15}$$

$$\frac{\mathrm{d}\hat{z}_1}{\mathrm{d}t} = \dot{x}_m - \frac{|\dot{x}_m|}{g(\dot{x}_m)} \hat{z}_1 + l_1 \tag{16}$$

The observer error equation is described by

$$\frac{\mathrm{d}\bar{z}_0}{\mathrm{d}t} = - \frac{|\dot{x}_m|}{g(\dot{x}_m)} \bar{z}_0 - l_0 \tag{17}$$

$$\frac{\mathrm{d}\bar{z}_1}{\mathrm{d}t} = - \frac{|\dot{x}_m|}{g(\dot{x}_m)} \bar{z}_1 - l_1 \tag{18}$$

where, $\bar{z}_0 = z - \hat{z}_0$, $\bar{z}_1 = z - \hat{z}_1$

$$\varepsilon = \dot{x}_m - (\dot{x} - \lambda e) \tag{19}$$

where, $e = x_m - x$, $\varepsilon = \dot{e} + \lambda e$.

By linking Eq. (19) with Eq. (14), the equation is described by

$$m_m \dot{\varepsilon} = F_{ph} - \sigma_0 z_0 + \sigma_1 \frac{|\dot{x}_m|}{g(\dot{x}_m)} z_1 - \sigma \dot{x}_m - k_{mk} x_m - m(\ddot{x} - \lambda \dot{e}) - F_{mk0} \tag{20}$$

The estimated value of σ_0, σ_1, σ is $\hat{\sigma}_0$, $\hat{\sigma}_1$, $\hat{\sigma}$, and the adaptive law is described by

$$m_m \dot{\varepsilon} = -k\varepsilon + \hat{\sigma}_0 \hat{z}_0 - \sigma_0 z_0 - \hat{\sigma}_1 \frac{|\dot{x}_m|}{g(\dot{x}_m)} \hat{z}_1 + \sigma_1 \frac{|\dot{x}_m|}{g(\dot{x}_m)} z_1 + \hat{\sigma} \dot{x}_m - \sigma \dot{x}_m \tag{21}$$

where, $k > 0$, $\bar{\sigma}_0 = \sigma_0 - \hat{\sigma}_0$, $\bar{\sigma}_1 = \sigma_1 - \hat{\sigma}_1$, $\bar{\sigma} = \sigma - \hat{\sigma}$, $\bar{z}_0 = z_0 - \hat{z}_0$, $\bar{z}_1 = z_1 - \hat{z}_1$.

Define the Lyapunov function for the system

$$V = \frac{1}{2} m_m \varepsilon^2 + \frac{1}{2} \sigma_0 \bar{z}_0^2 + \frac{1}{2} \sigma_1 \bar{z}_1^2 + \frac{1}{2r_0} \bar{\sigma}_0^2 + \frac{1}{2r_1} \bar{\sigma}_1^2 + \frac{1}{2r_2} \bar{\sigma}^2 \tag{22}$$

where, r_0, r_1, r_2 is the adaptive gain, r_0, r_1, $r_2 > 0$.

$$\dot{V} = -k\varepsilon^2 - \sigma_0 \frac{|\dot{x}_m|}{g(\dot{x}_m)} \bar{z}_0^2 - \sigma_1 \frac{|\dot{x}_m|}{g(\dot{x}_m)} \bar{z}_1^2 - \bar{\sigma}_0 \left(\varepsilon \hat{z}_0 + \frac{1}{r_0} \dot{\hat{\sigma}}_0 \right) - \bar{\sigma}_1 \left(\frac{1}{r_1} \dot{\hat{\sigma}}_1 - \varepsilon \frac{|\dot{x}_m|}{g(\dot{x}_m)} \bar{z}_1 \right) - \bar{\sigma}_0 \left(\varepsilon \dot{x}_m + \frac{1}{r_2} \dot{\hat{\sigma}} \right) - \sigma_0 \bar{z}_0 (\varepsilon + l_0) + \sigma_1 \bar{z}_1 \left(\varepsilon \frac{|\dot{x}_m|}{g(\dot{x}_m)} - l_1 \right) \tag{23}$$

The control rate is described by

$$\dot{\hat{\sigma}}_0 = - r_0 \varepsilon \hat{z}_0 \tag{24}$$

$$\dot{\hat{\sigma}}_1 = r_1 \varepsilon \hat{z}_1 \frac{|\dot{x}_m|}{g(\dot{x}_m)} \tag{25}$$

$$\dot{\hat{\sigma}}_1 = - r_2 \varepsilon \dot{x}_m \tag{26}$$

$$l_0 = - \varepsilon \tag{27}$$

$$l_1 = \varepsilon \frac{|\dot{x}_m|}{g(\dot{x}_m)} \tag{28}$$

By linking Eq. (20) with Eqs(21) – (25), the

equation is described by

$$\dot{V} = -k\varepsilon^2 - \sigma_0 \frac{|\dot{x}_m|}{g(\dot{x}_m)}\bar{z}_0^2 - \sigma_1 \frac{|\dot{x}_m|}{g(\dot{x}_m)}\bar{z}_1^2 \quad (29)$$

where, $k > 0$, $\sigma > 0$, $\sigma_0 > 0$, $\sigma_1 > 0$, $g(\dot{x}_m) > 0$, $|\dot{x}_m| \geqslant 0$.

$\dot{V} \leqslant 0$, the matrix is negative semi-definite, and the closed-loop system is asymptotically stable.

Therefore, according to the Lyapunov theorem, the adaptive control rate can guarantee global stability for the system.

3 Parameters identification of the friction model

Through the method of experimental identification, the static and dynamic parameters of the LuGre friction model are obtained.

3.1 The static parameters identification of the friction model

When the system works in steady state ($dz/dt = 0$), by Eq. (13), static friction F_{fss} is described by

$$F_{fss} = p_L A_m - k_{mk} x_m - F_{mk0} \quad (30)$$

The main valve core moves in different speed $\{v\}_{i=1}^{N}$ with velocity closed-loop control, the static friction $\{F_{fss}\}_{i=1}^{N}$ is obtained by Eqs(10) ~ (12), and the relation between static friction and velocity is determined, namely the Stribeck. So, the static friction parameters F_s, F_c, v_s and σ_2 are estimated by the physical meaning of the Stribeck. Fitting the test results with the least square method, the results are shown in Fig. 4 and Fig. 5, the static friction parameters are shown in Table 1.

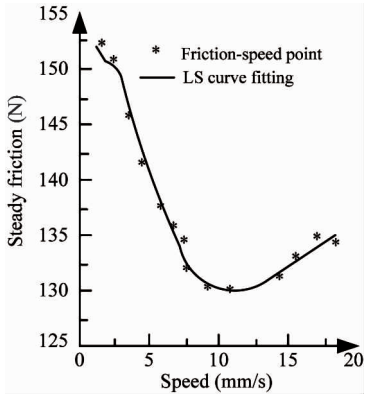

Fig. 4 Fitting curve of the static friction model in positive direction

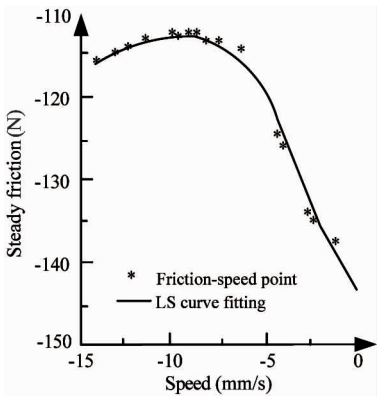

Fig. 5 Fitting curve of the static friction model in negative direction

Table 1 Identification parameters of the LuGre static friction model

Direction	The static parameters			
	F_s (N)	F_c (N)	v_s (mm/s)	σ_2 (N/(mm/s))
Positive	151.0767	122.1845	10.69	0.5475
Negative	-141.0647	-102.6461	-9.89	0.5475

3.2 Dynamic parameters identification of the friction model

In the region of the static friction at low speed, the main valve has no apparent movement, and the friction type is the coulomb friction. $z \approx x_m$, $dz/dt \approx \dot{x}_m$, by Eq. (10), the main valve friction F_{mf} is described by

$$F_{mf} \approx \sigma_0 x_m + (\sigma_1 + \sigma_2)\dot{x}_m \quad (31)$$

When the motion stops

$$\sigma_0 \approx \frac{F_{mc}\mathrm{sgn}\dot{x}_m}{x_s} \quad (32)$$

where, x_s is the steady-state displacement in the region of static friction.

Based on the identification results, $x_s = 0.04029$mm is obtained by a small step signal response, then σ_0 is got.

$$A_m p_L = m_m \ddot{x}_m + (\sigma_1 + \sigma_2)\dot{x}_m + (k_{mk} + \sigma_0)x_m \quad (33)$$

By applying the Laplace transform, Eq. (34) is described by

$$G(s) = \frac{1}{m_m s^2 + (\sigma_1 + \sigma_2)s + k_{mk} + \sigma_0} \quad (34)$$

$$G(s) = \frac{\omega_n^2}{s^2 + 2\xi\omega_n s + \omega_n^2} \quad (35)$$

where, ω_n is the natural frequency of second-order oscillation, ξ is the damping ratio of second-order oscilla-

tion, the best damping ratio is 0.7.

By linking Eq. (34) with Eq. (35), the function is described by

$$\sigma_1 + \sigma_2 = 2\xi \sqrt{m_m(k_{mk} + \sigma_0)} \quad (36)$$

By linking Eq. (33) with Eq. (36), the dynamic friction parameters as shown in Table 2.

Table 2 The identification parameters of the LuGre dynamic friction model

Direction	The dynamic parameters	
	σ_0 (N/mm)	σ_1 (N/(mm/s))
Positive	3035.00	0.6854
Negative	3035.00	0.6854

4 Simulation and experimental analysis of the friction compensation

4.1 Joint simulation model for the friction compensation

The joint simulation model of AMESim and MATLAB/Simulink for the piloted large diameter electro-hydraulic proportional valve is shown in Fig. 6.

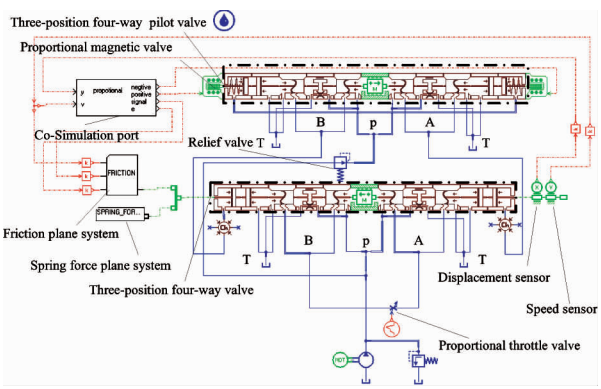

Fig. 6 Joint simulation model of AMESim and MATLAB/Simulink

4.2 The simulation analysis of the friction compensation

The low speed crawl phenomenon of the main valve turns up in the process of low speed movement. The paper contrasts the friction compensation effect of the feed-forward compensation and the adaptive compensation. The displacement of main valve core and error response to the sine input ($y = 7.5 \times 10^{-3} \sin 0.1\pi$) are shown in Fig. 7 and Fig. 8.

As shown in Fig. 7 and Fig. 8, the low speed crawl phenomenon of the main valve core is basically eliminated to the sine input. Under the feed-forward compensation control, the steady-state error is [-1.51×10^{-4}m, 0.76×10^{-4}m]. The friction compensation has a better effect. However, the main valve reversing

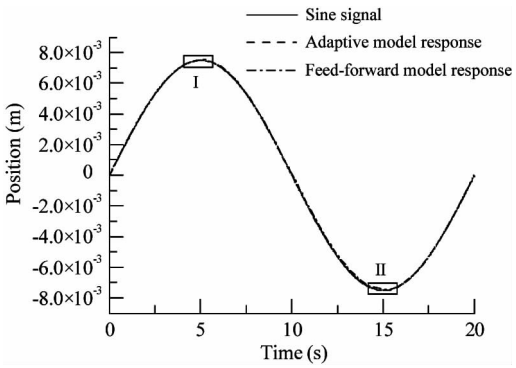

Fig. 7(a) The response to the sine input

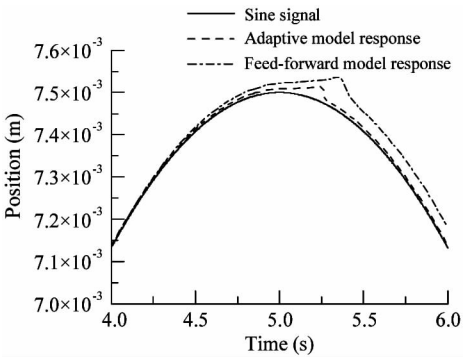

Fig. 7(b) The enlarged drawing of Ⅰ

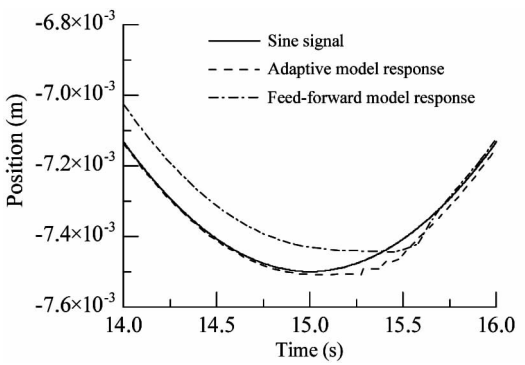

Fig. 7(c) The enlarged drawing of Ⅱ

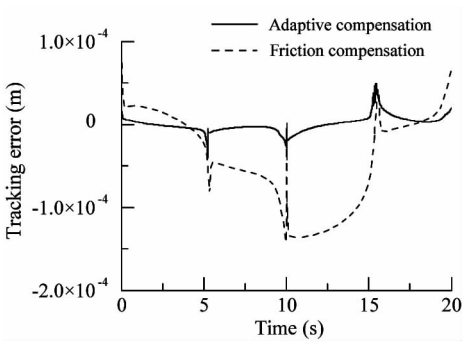

Fig. 8 The error curve

in the full scale position, the polarity of the proportional valve has not changed. The main valve high pressure is reduced to the level of the passivity force with the corresponding throttle, and the valve core gets to the

dynamic force balance. Therefore, the main valve has a sensitive area, and forms the phenomenon similar to a "flat top". At the same time, due to the "dead zone", the biggest tracking error appears at 10s.

The adaptive friction compensation tracking performance is obviously better than the friction feed-forward compensation, its steady-state error is near zero, about $[-4.23\times10^{-5}\text{m}, 5.91\times10^{-5}\text{m}]$. The position tracking accuracy is higher, and the lag time of the main valve through the dead zone is shorter than the feed-forward compensation control. By analyzing the effect of the friction compensation method, the adaptive compensation based on LuGre friction model has obvious advantages in terms of friction compensation, which greatly improves the low speed tracking performance of the position control system.

4.3 The experimental analysis of the adaptive friction compensation

The nonlinear friction compensation hydraulic principle diagram and test bed are shown in Fig. 9 and Fig. 10.

The friction characteristics change along with the change of system operation conditions and environment, and the friction model parameters changes as well. It is very difficult to achieve satisfactory effect for the feed-forward compensation with fixed parameters. The adaptive friction compensation is combined with friction model parameters estimation and adaptive friction compensation controller, the changes of the friction model parameters and the object system model

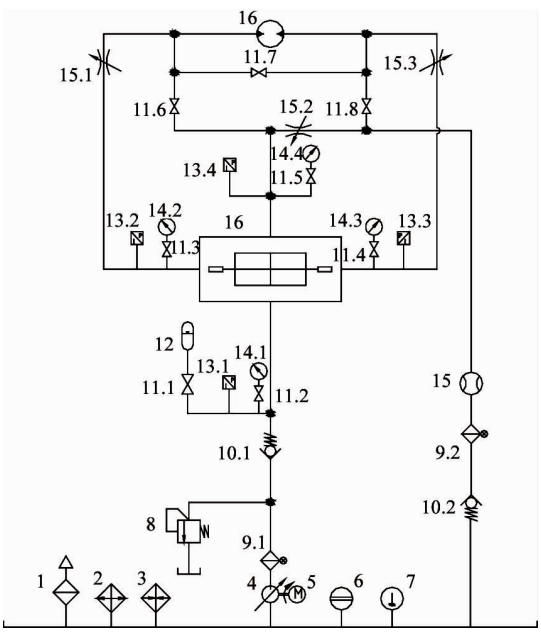

Fig. 9 The hydraulic principle diagram of the proportional valve test bed

Fig. 10 The test bed of the proportional valve

parameters can be compensated in real time. It achieves satisfactory compensation effect and meets the requirements of control accuracy, experiment curves of which are shown in Fig. 11 and Fig. 12.

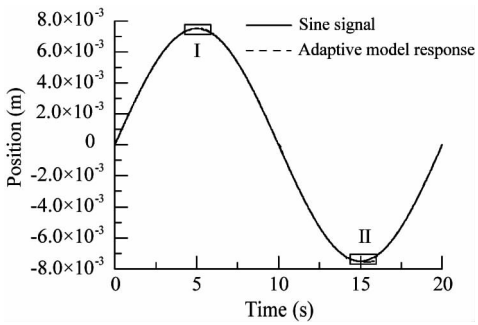

Fig. 11(a) The response to the sine input

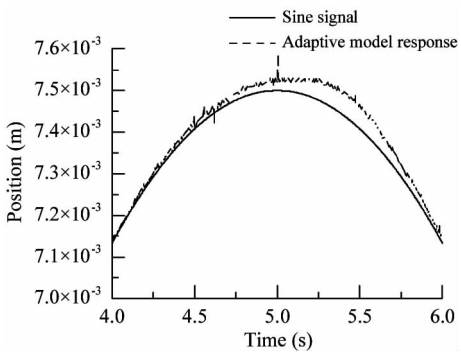

Fig. 11(b) The enlarged drawing of Ⅰ

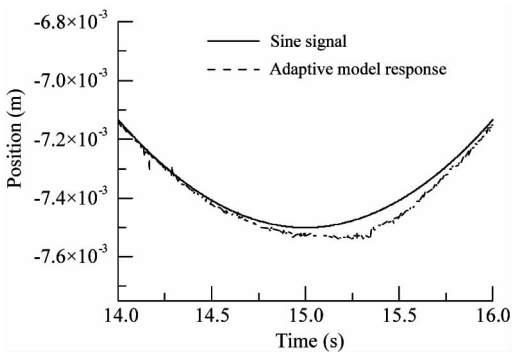

Fig. 11(c) The enlarged drawing of Ⅱ

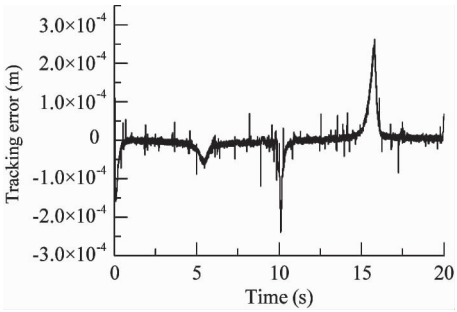

Fig. 12 The error curve

As shown in Fig. 11 and Fig. 12, the actual location tracking is essentially overlapped with the given position under the adaptive friction compensation, its steady-state error is near zero, about $[-2.4\times10^{-4}\text{m}, 2.6\times10^{-4}\text{m}]$. The experiment results and simulation results have certain difference due to the change of oil temperature, oil elastic modulus, abrasion of valve core and so on in experiment. The result of the experiment still proves that the adaptive friction compensation method can effectively compensate for the negative effects of nonlinear friction. It is able to achieve location tracking quickly with good stability. Compared with the feed-forward friction compensation method, the compensation effect is better, and it is suitable for high precision positioning control and frequent reversing conditions.

5 Conclusion

Based on the Lyapunov stability the adaptive law of the friction parameters is designed, and the adaptive compensation model based on LuGre friction model is built. The accurately joint simulation model of large diameter electro-hydraulic proportional valve is established, and the effectiveness of the friction nonlinearity compensation strategy is analysed.

The adaptive friction compensation based on LuGre friction model gives full consideration to the dynamic friction problem of large diameter electro-hydraulic proportional valve core. The adaptive friction compensation method can accurately compensate for the negative effects of nonlinear friction, and it is able to achieve location tracking quickly with good stability. It is a feasible solution to improve the dynamic control performance of large diameter electro-hydraulic proportional valve.

References

[1] Miao Z Y, Xu S L, Min L Y. The view of high-frequency electrohydraulic propotional servo valve. *Chinese Hydraulics & Pneumatics*, 2012, (3): 98-100

[2] Dasgupta K, Watton J. Dynamic analysis of proportional solenoid piloted relief valve by bond-graph. *Simulation Modelling Practice and Theory*, 2005, 13: 21-38

[3] Wang R J, Mei Z Q, Li X G, et al. Research on adaptive nonlinear friction compensation of mechatronic servo. *Systems Proceeding of the CSEE*, 2012, 32(36): 123-129

[4] Swlmic R R, Lewis F L. Neural network approximation of piecewise continuous functions: application on friction compensation. *IEEE Transactions on Neural Networks*, 2002, 13(3): 745-751

[5] Armstrong H B, Dupont P, Canudas D W C. Survey of models, analysis tools and compensation methods for the control of machines with friction. *Automatica*, 1994, 30(7): 1083-1138

[6] Miao Z H, Li Z H, Wang X Y, et al. Modeling and friction dynamic compensation for ultra-large-diametered hollow hydraulic motor servo system. *Transaction of Chinese Society for Agricultural Machinery*, 2013, 44(12): 314-320

[7] Armstrong B, Neevel D, Kusik T. New result in NPID control: tracking, integral control, friction compensation and experimental result. In: Proceedings of the 1999 IEEE International Conference on Robotics & Automation, Detroit Michigans, USA, 1999. 837-842

[8] Friedland B, Park Y J. On Adaptive Friction Compensation. *IEEE Transactions on Automatic Control*, 1992, 37(10): 1609-1612

[9] Yazdlizadeh A, Khorasani K. Adaptive friction compensation based on the Lyapunov scheme. In: Proceedings of the IEEE International Conference on Control Applications, Hawaii, USA, 1996. 863-867

[10] Liu L L, Liu H Z, Yuan D N, et al. Modal parameter identification of time varying vibration systems subjected to stick-slip friction. *Ransaction of Chinese Society for Agricultural Machinery*, 2010, 41(1): 177-181

[11] Freidovich L, Robertsson A, Shiriaev A, et al. LuGre model based friction compensation. *IEEE Transactions on Control Systems Tecnology*, 2010, 18(1): 194-200

[12] Xie F X. Sliding-mode-observer-based adaptive control for servo actuator with friction. *IEEE Transactions on Industrial Electronics*, 2007, 54(3): 1517-1527

[13] Xiang H B, Tan W B, Li X F, et al. Adaptive friction compensation based on LuGre model. *Journal of Mechanical Engineering*, 2012, 48(17): 70-74

[14] Lee T H, Tan K K, Huang S. Adaptive friction compensation with a dynamical friction model. *IEEE/ASME Transactions on Mechatronics*, 2011,16(1): 133-140

[15] De Wit C C, Olsson H, Astrom K J, et al. A new model for control of system with friction. *IEEE Transactions on Automatic Control*, 1995, 40(3):419-425

Kong Xiangdong, born in 1959. He received his Ph. D degrees in Metallurgical Mechanics Department of Northeast Heavy Machinery Institute (Yanshan University) in 1991. He also received his B. S. degree from Zhejiang University in 1982 and received his M. S. degree from Northeast Heavy Machinery Institute in 1985. His research interests include the fluid transmission and control, the design and optimization of hydraulic component.